Gas-phase composition measurements during chlorine assisted chemical vapor deposition of diamond: A molecular beam mass spectrometric study

C. A. Rego,[a] R. S. Tsang,[b] P. W. May, M. N. R. Ashfold, and K. N. Rosser
School of Chemistry, University of Bristol, Cantock's Close, Bristol BS8 1TS, United Kingdom

(Received 13 November 1995; accepted for publication 16 January 1996)

We have constructed a molecular beam mass spectrometer designed specifically to sample gases from a diamond chemical vapor deposition (CVD) process chamber thereby enabling characterization of the gas-phase CVD environment. With this *in situ* diagnostic technique we have obtained quantitative measurements of the composition of the gas-phase species as a function of filament temperature for a variety of C/H/Cl gas mixtures. The precursor mixtures used were 1% of a chloromethane ($CH_{4-n}Cl_n$, n=1-4) in hydrogen and 1% CH_4 in hydrogen with added Cl_2 varying from 1% to 4%. At filament temperatures optimum for diamond growth ($\sim$2300°C) the relative $CH_4/C_2H_2/C_2H_4$ product distribution measured in the gas mixture is remarkably similar to that established when CH_4 is the carbon precursor species. At these filament temperatures almost all the chlorine is reduced to HCl, its concentration being proportional to the Cl fraction in the source gas, regardless of the form of the chlorine in the source gas mixture. Compositional analysis of the as-grown diamond films indicated that no chlorine was present in the bulk of the films, though trace amounts of chlorine were detected on the film surface. From these observations we surmise that chlorine atoms are involved in the gas-surface reactions which produce active growth sites on the diamond surface. © *1996 American Institute of Physics.* [S0021-8979(96)08808-X]

I. INTRODUCTION

High quality diamond films can be grown by chemical vapor deposition (CVD) using a variety of methods to activate the process gas mixture, e.g., hot filament and microwave, rf and dc plasmas.[1,2] Typically any hydrogen/hydrocarbon source gas mixture may be used subject to the C/H ratio being less than $\sim$0.03. Common to each deposition method and source gas mixture employed in the synthesis of CVD diamond is the requirement of high gas temperatures which generates atomic hydrogen and produces reactive carbon species. Recent gas phase composition studies[3–5] have shown that, for gas temperatures in excess of $\sim$2000°C and a given C/H proportion, the hydrocarbon source gas is dissociated to the extent that the relative concentrations of the active carbon species are remarkably insensitive to the particular choice of hydrocarbon feedstock gas. To date models of the reaction mechanisms by which different hydrocarbon precursors are able to produce high quality CVD diamond have focused on methyl (CH_3) radicals[6,7] and/or acetylene (C_2H_2)[8,9] as the active carbon species in the growth process.

Successful diamond growth may also be achieved using either oxygen containing source gases, e.g. CH_3OH[10] and CO,[11] in excess H_2 or by the addition of small amounts of O_2[12] to the standard hydrocarbon/H_2 source gas mixture. The presence of gas phase oxygen can enhance diamond growth rates and also enable diamond synthesis at lower substrate temperatures. A survey of the different C/H/O source gas mixtures used to produce diamond films is summarized in the well known phase diagram of Bachmann *et al.*[13] The apparent catalytic effect of oxygen in the CVD process enabling diamond growth at substrate temperatures lower than the standard ($\sim$900°C) has possible important implications for coating lower melting point materials such as aluminium, or materials that are unstable at high temperatures in the reducing atmosphere typical of the CVD process. Such advantages cannot be fully exploited in hot filament CVD (HFCVD) reactors, though, because the presence of oxygen rapidly degrades the heated filament. A similar catalytic effect has been demonstrated[14–20] when halogen species are present in the gas phase, though the precise reaction mechanisms have not been studied in detail: this is the subject of the present work.

One study,[14] using monosubstituted halocarbons CH_3F, CH_3Cl, CH_3Br or CH_3I in H_2 as the input gas mixture in a hot filament reactor, showed that with CH_3Cl the diamond growth rates increased relative to those found using CH_4 as the precursor. It was concluded that the increased reactivity of CH_3Cl compared to the other methyl halides stems from the difficulty, in the one case, of forming atomic fluorine from CH_3F and, at the other extreme, the inability of Br and I atoms to abstract terminating hydrogen atoms from the growing diamond surface. Other studies using chloride source gases (CH_3Cl, CH_2Cl_2, $CHCl_3$ and CCl_4) both in hot filament reactors[15,16] and in microwave plasmas[17,18] have also shown that chloromethanes produce a slightly higher diamond growth rate than with methane at normal substrate temperatures ($\sim$900 °C), and all indicate that this difference is more pronounced at lower substrate temperatures. Recently,[19] a study using chlorine with typical $H_2/Cl_2/CH_4$ ratios of 100/5/1 demonstrated that similar growth rates can be achieved at substrate temperatures $\sim$150°C lower than that found for typical H_2/hydrocarbon gas mixtures, and that

[a]Present address: Department of Chemistry, The Manchester Metropolitan University, Chester Street, Manchester M1 5GD, U.K.
[b]Electronic mail: r.s.tsang@bris.ac.uk

 0021-8979/96/79(9)/7264/10/$10.00

TABLE I. Bond dissociation energies.[a]

Bond	Bond strength /kJ mole^{-1}
H-H	432
Cl-Cl	239
H-Cl	428
H-F	564
H-CH_3	435
Cl-CCl_3	305
Cl-$CHCl_2$	331
Cl-CH_3	352
F-CF_3	540

[a]See Reference 21.

the addition of a few percent of HCl to the standard CH_4/H_2 mixture could cause a tenfold enhancement in growth rates at 670 °C.[20]

A number of possible gas phase and gas-solid heterogeneous reaction mechanisms have been suggested for the apparent catalytic activity of chlorine in the CVD process. The C-Cl bond strengths in the various chloromethanes are weaker than the C-H bond in methane (see Table I) so rupture of the C-Cl bond, by reaction with H atoms, can be achieved more readily to produce active methyl or chloromethyl ($CH_{3-n}Cl_n$, n=1-3) radicals. The latter species have been suggested as being more effective growth precursors than methyl[14] because of the possibility of facile surface dehydrochlorination reactions.[15] Alternatively, the catalytic properties of chlorine in the CVD process may be due to reactions with terminal C-H at the diamond surface, or the possibility of forming surface bonded C-Cl. The terminating H and Cl atoms essentially serve the same purpose in suppressing formation of sp^2 bonding at the growing surface at high substrate temperatures. Abstraction of surface Cl atoms by atomic H, or removal of surface adsorbed H by atomic chlorine, has a significantly lower activation energy than H abstraction of surface H thereby enabling active surface sites to be created at lower substrate temperatures.[20]

In order to identify and understand the gas-phase and gas-solid reaction mechanisms in the CVD process, and the changes in the reactions which occur when chlorine is present, quantitative measurement of the concentrations of both *free radical* and *stable* species in the gas phase are required, with minimal perturbation of the process environment. A number of *in situ* diagnostic techniques are available for such measurements. Optical spectroscopy[1] is a widely used technique, but is generally specific to a particular target species. Gas chromatographic[3,22] and mass spectrometric[23–26] studies have the advantages of generality and the fact that many stable species can be analyzed simultaneously, though recombination in the probe used to sample the process gas in these studies precludes detection of reactive gas species. However, with careful design of the gas sampling system, mass spectrometry can be used to detect free radicals. Molecular beam mass spectrometry (MBMS) of the diamond growth environment in both hot filament and microwave plasma reactors by Hsu and co-workers[27–29] has enabled quantitative measurement of the concentrations of H atoms and CH_3 radicals as well as stable species like CH_4, C_2H_2, etc.

In this article we present a full description of the design of our MBMS gas phase diagnostic system and of the data collection and reduction procedures which enable the determination of the mole fractions of both the stable neutral and free radical species prevalent at different conditions in the HFCVD process. We then use the MBMS to characterize the gas phase environment, and its variation with filament temperature, when chlorine containing precursors $CH_{4-n}Cl_n$ ($n=1-4$) in H_2 and $CH_4/Cl_2/H_2$ mixtures are input as the source gases. Such information provides insight into the gas-phase chemical kinetics prevalent in the CVD process. We also wish to understand this behavior in terms of changes in the gas-phase chemistry and/or the different gas-solid heterogeneous reactions when chlorine is present in the gas mixture.

II. EXPERIMENT

The deposition chamber was a standard HFCVD reactor consisting of a stainless steel six-way cross and employing a 0.25 mm thick, coiled tantalum filament to activate the gas mixture. In the present study we replaced methane, the most commonly used hydrocarbon precursor gas, with (1) a range of different halomethanes taking care to always maintain a carbon-to-H_2 ratio of 1:100 in the gas mixture, (2) a gas mixture containing 1% CH_4 in Cl_2/H_2, the amount of chlorine varying from 0.5% to 4% (1–8 at. %). The gas flows were governed by calibrated mass flow controllers (Tylan General) and the total gas pressure was maintained at 20 Torr during the film growth. Films were deposited on silicon (100), which had been previously manually abraded with 1–3 μm diamond powder, under standard growth conditions: substrate temperature 900°C, filament temperature 2300°C, filament-substrate distance 4 mm.

Gas-phase product distributions were monitored as a function of the filament temperature using a mass spectrometer system described below. Filament temperatures were measured using a two-color optical pyrometer (Land Infrared) and the filament to sampling-orifice distance held at 4 mm for all readings. The absolute concentrations of the species monitored are determined by direct room temperature calibration with mixtures of known composition. A full description of the calibration procedures is given in section III.

A. Molecular beam mass spectrometer design

The design of the two-stage MBMS is optimized to sample from a filament assisted CVD process chamber operating at a pressure of ~20 Torr. Minor modifications have been made to our standard process chamber so that the substrate and filament assembly can move in the x,z plane (see Fig. 1) relative to the MBMS sampling orifice, thus enabling spatial distribution studies.[30] The schematic diagram of the CVD chamber coupled to the MBMS sampling system, shown in Fig. 1, indicates that in this study we do not sample gas *via* an orifice in the substrate: the sampling cone arrangement is positioned so as to sample the process gas mixture at the same radial distance from the filament as the substrate surface.

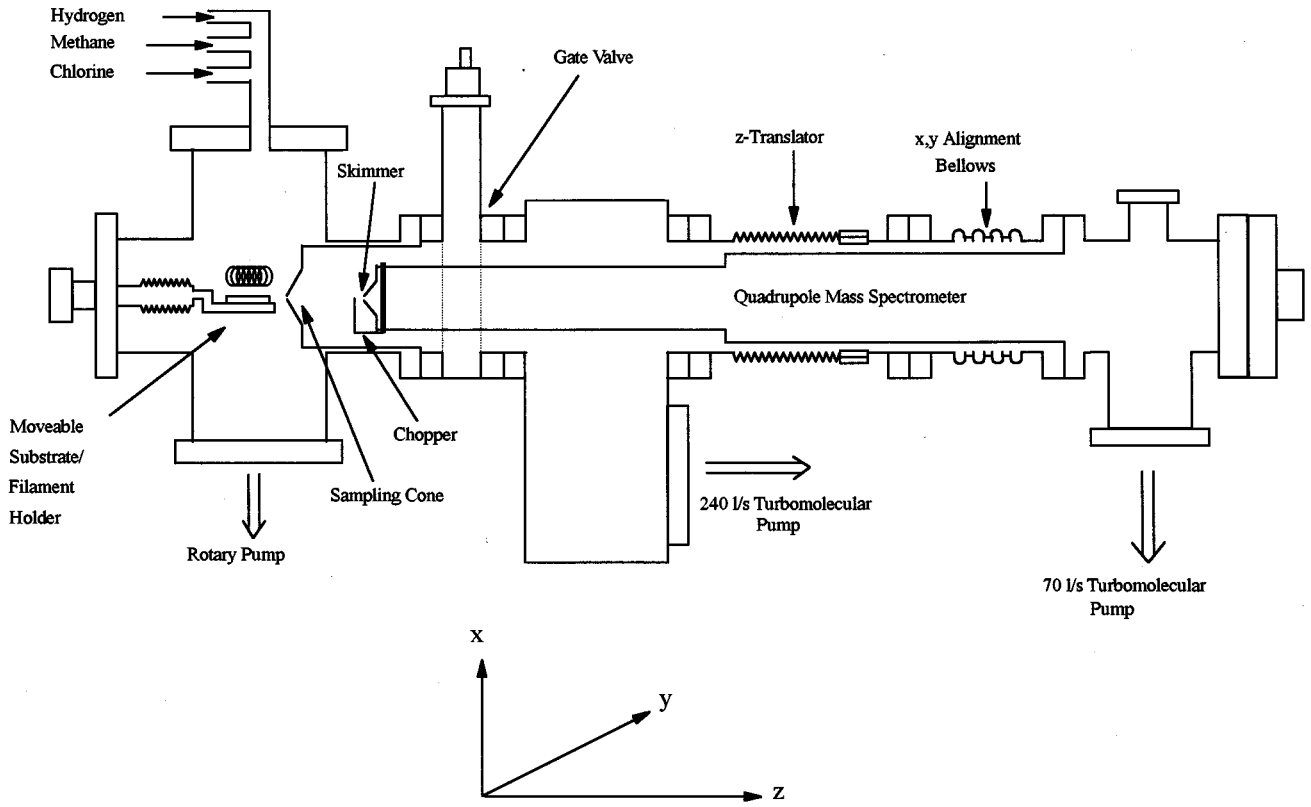

FIG. 1. Schematic diagram of the molecular beam mass spectrometer coupled to the hot filament CVD reactor.

Gas from the process chamber is extracted through a 100 μm diameter orifice in a stainless steel sampling cone. The sampled gas is collimated by a second 1 mm diameter skimmer and has an unobstructed path to the electron ionization chamber of a HAL/3F PIC 100 quadrupole mass spectrometer (Hiden Analytical, Warrington, England). Since the process pressure is typically 20 Torr and the mass spectrometer can only operate at pressures below 10^{-6} Torr, differential pumping is required. Our two stage system uses turbomolecular pumps, the pumping speed being 240 ℓ/s in the first stage and 70 ℓ/s in the high vacuum MS chamber. The pressure in each stage during gas sampling is typically 10^{-3} Torr and 5×10^{-7} Torr respectively. The diameter of the extraction orifice and collimating skimmer are selected to match the gas influx from the CVD chamber with the gas throughput of the turbomolecular pumps.

A z-translator consisting of an edge-welded bellows assembly allows the distance from the skimmer to the extraction orifice to be varied. A near linear increase in the detected signals results as the skimmer to extractor distance is reduced to about 2 cm. However, if the skimmer is moved closer than this optimum distance the pumping speed near the orifice is reduced, becoming conductance limited, and causing the background pressure to increase so nullifying any benefit. There is a gate valve between the process chamber and the MBMS system so that the MS can be withdrawn and isolated from the process chamber when the latter is vented to atmosphere. The system also incorporates an x,y-manipulator in order to align the MS skimmer with the molecular beam, thereby ensuring maximum sensitivity.

The signal detected by the mass spectrometer is proportional to the sum of the background gas and the gas introduced by the molecular beam. In order to quantify the free radical concentrations the two components need to be distinguished and the background effects eliminated. This is achieved by modulating the molecular beam using a piezoelectrically driven vibrating reed chopper located between the sampling orifice and the collimating skimmer, some 5 mm from the MS skimmer. An opto-reflective switch monitors when the chopper is in resonance and measures the resonant frequency ($\sim$50 Hz). Synchronized TTL signals are sent to the MS software which control pulse gating to the MS counter. The width of the signal counting window is variable and is set to 2 ms allowing the signal to be collected only when the path of the molecular beam to the ionization source is fully obstructed or unobstructed. This enables the background signal component to be eliminated from the total signal, thus allowing quantitative analysis for the radical species.

Since the actual electron energy in the ionization source in the MS is not necessarily the same as the potential applied to the cathode filament, the energy scale needs to be calibrated. The true MS cathode voltage was determined by measuring the ionization potential (IP) of Ar and correcting to its literature value of 15.76 eV. We note that there is a small spread in the electron kinetic energy distribution (FWHM $\sim$1 eV) which affects the accuracy of the linear extrapolation method. All cathode electron energies quoted

in this article have had the calibration correction applied and are accurate to within 0.5 eV.

III. DATA COLLECTION AND REDUCTION

A. MS calibration

When measuring the signal for species with a particular mass-to-charge (m/e) ratio it is important to eliminate or at least minimize interference from unwanted ions with the same (m/e) or those arising from fragmentation of other ionic species. This can be achieved if it is possible to measure the signal of the species of interest at an electron ionization energy just below the ionization threshold of the interfering species. For example, we can detect the signal for C_2H_4 (m/e = 28, IP = 10.51 eV) using an electron energy of 13.5 eV, thus minimizing signal interference from CO (IP =14.0 eV) and N_2 (IP = 15.55 eV). However, in cases where interference from fragmentation is unavoidable (e.g. detection of C_2H_4 in the presence of C_2H_6) corrections to the signals have to be made using measured fragmentation patterns. In the present work detection of all stable carbon and chlorine containing species, other than C_2H_4, was made with an ionizing electron energy of 15.5 eV.

The relationship between the signal intensity of a given species, I_i, measured at a given electron energy, E_i, and its mole fraction, X_i, is given by

$$I_i(E_i) = S_i X_i, \tag{1}$$

where the sensitivity factor, S_i, depends on the ionization cross section of i and the MS gas sampling efficiency, which may vary for different gas species and the local temperature, pressure and composition of the gas sample. The concentrations of the stable species are determined by direct room temperature calibration of mixtures of known composition ensuring that, for each species monitored, we use the same user selected (see above) electron ionization energy in both calibration and data collection cycles and that the total process pressure remains constant. However, we find that an additional temperature dependent correction also needs to be made (see Sec. III B).

This simple calibration procedure is justified for small concentrations of C/Cl containing species ($<1\%$) in hydrogen on the grounds that, for heavy species diluted in a large excess of hydrogen, the transport of the process gas through the sampling orifice and subsequent formation of a supersonic molecular beam are dominated by the mass transport properties of the hydrogen. However, problems arise with this calibration procedure when the concentration of a particularly heavy species, such as Cl_2, in the gas mixture is significantly greater than $\sim 1\%$. This is illustrated in Fig. 2 which shows the attenuation of the CH_4 signal when different amounts of chlorine are added to a 1% CH_4 in H_2 mixture, an example chosen because of its relevance to our studies. In these cases calibration was carried out using known amounts of target gas of interest (e.g. CH_4, C_2H_2, HCl, etc.) diluted in the appropriate H_2/Cl_2 mixture. This signal attenuation could, in principle, be due to CH_4 reacting with the added Cl_2 at room temperature or be a consequence of mass discrimination effects in the molecular beam; such effects on MBMS sampling efficiency are well known.[27] Evidence to support the latter explanation, i.e. that the light CH_4 molecules are preferentially excluded from the center of the beam by the heavy Cl_2 molecules comes from the equivalent experiments in which we replace the 1% CH_4 by 1% Ne. The Ne signal is observed to fall off in a similar way.

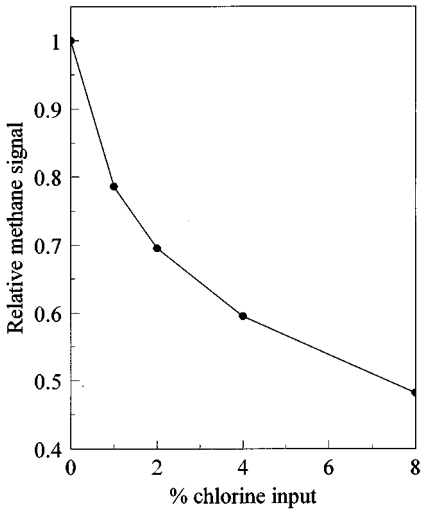

FIG. 2. Variation of measured CH_4^+ signal as a function of gas composition. The signal for 1% CH_4 in H_2 is attenuated as the chlorine concentration in the gas mixture increases.

Detection of low concentrations of free radicals (e.g. CH_3 in a large excess of CH_4 or CH_3Cl) requires the use of the threshold ionization technique which distinguishes ions generated by direct electron impact of the radicals from those generated by dissociative ionization of the parent molecule. Application of this technique for the detection of methyl radicals, for example, requires the electron energy of the MS ionization source to be maintained well above the ionization threshold of the CH_3 radicals (IP = 9.84 eV), in order to maximize the detection sensitivity, yet sufficiently below the appearance potential (AP) of CH_3^+ from the dissociative ionization of CH_4 (14.3 eV). Signal interference from the parent molecule is thereby minimized. In practice, all CH_3^+ signal measurements were made using an ionizer voltage centered at 13.5 eV, which resulted in a limited amount of fragmentation of the parent species but was readily corrected using measured fragmentation data.

In order to quantify the radical species we need to distinguish between the beam and background components of the MS signal since most of the radical species in the background component do not survive to be detected. We achieve this by modulating the beam as described in section II. The dependence of the CH_4^+ signal with chopper delay (Fig. 3) shows that $\sim 35\%$ of the total signal comes from species in the molecular beam.

Ideally we would eliminate the background components for all our measurements, thereby enabling the signal intensities of each species to be directly related to their ionization cross sections. However, the restricted mechanical pumping speed of our MBMS system precludes such a procedure because of limitations in sensitivity of the system when modulating the beam. Instead, in order to correct for the destruc-

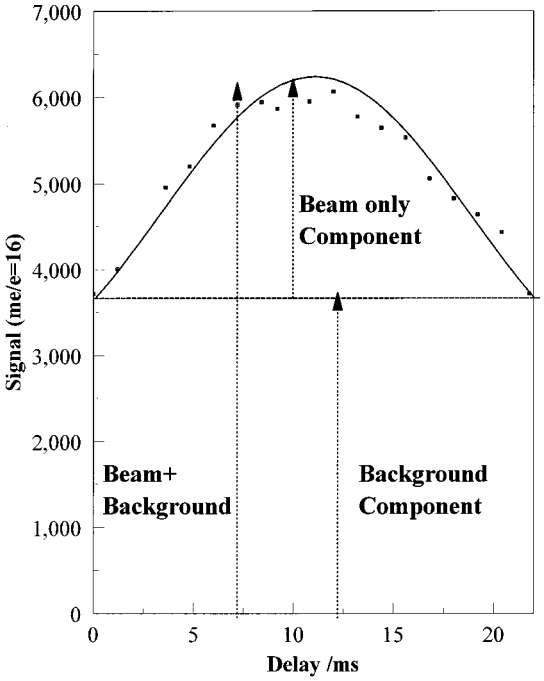

FIG. 3. Illustrative diagram showing how the measured CH_4^+ signal varies as a function of the chopper delay. This indicates that only ~35% of the total signal comes from species in the molecular beam. The smooth curve through the points is included to guide the eye.

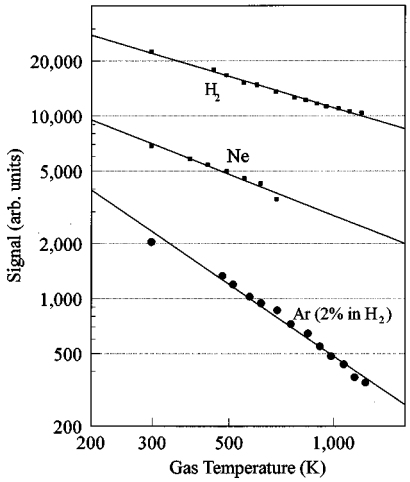

FIG. 4. Variation of the detected signal as a function of the local temperature of the gas being sampled. For pure gases (H_2 and Ne shown) the fit to the experimental data show a near $T^{-0.6}$ dependence. For 2% Ar in H_2 the Ar signal shows a $T^{-1.6}$ dependence.

tion of CH_3 in the background we measured the proportion of the CH_4 in the beam and background components (Fig. 3) and ratio the CH_3 signal assuming that the CH_3 radicals are similarly partitioned between beam and background but that none of the radical species in the background gas survive to the detector; our ''corrected'' CH_3 signal is thus an upper limit.

Having corrected for loss of CH_3 in the background we can now directly calibrate for CH_3 by using measured ionization cross sections, Q, for methane[31] and methyl radicals,[32] at their respective electron energies used for detection, and the previously measured relationship between the CH_4 signal intensity and its mole fraction, *via*

$$\frac{X_{CH_3}}{X_{CH_4}} = \frac{I_{CH_3}(E_{CH_3})Q_{CH_4}(E_{CH_4})}{I_{CH_4}(E_{CH_4})Q_{CH_3}(E_{CH_3})}. \tag{2}$$

In such a calibration procedure we assume that the mass discrimination factors for CH_4 and CH_3 in excess H_2 on formation of the beam are equal.

B. Temperature dependence of MS sampling efficiency and thermal diffusion effects

Using pure H_2 at 20 Torr, the variation of I_{H_2} as a function of the local temperature, T, of the gas being sampled, as measured using a K-type thermocouple placed adjacent to the sampling orifice, shows a $T^{-0.6}$ dependence (see Fig. 4). Similar experiments using pure samples of He ($m/e=4$), Ne ($m/e = 20$) and Ar ($m/e = 40$) reveal that S_i shows the same temperature dependence for all these pure gases. In our results we assume a similar temperature dependence to the mass spectrometer sampling efficiency for all the hydrocarbon species of interest, and correct accordingly (by reference to the attenuation of the measured H_2 signal). This assumption is again justified on the grounds that, for small concentrations of heavy species in hydrogen, the mass transport properties are dominated by those of the hydrogen.

For a two component gas mixture the temperature dependence of the detected ion signals is different from that measured for a pure gas. For example, Fig. 4 shows that the Ar^+ signal measured for a two component, 2% Ar in H_2, gas mixture has a much greater temperature dependence ($\sim T^{-1.6}$) than that for a pure gas. This indicates an additional thermal effect for a gas mixture whereby a temperature gradient induces preferential diffusion of the heavier component in the mixture away from the higher temperature filament/sampling orifice region. This thermal diffusion (also known as the Soret effect[33]) has a major effect on the total concentration of carbon and halogen containing species measured in the region of the hot filament (see section IV). In the following section the absolute species concentrations measured 4 mm from the filament are presented with no additional adjustment being made for the depletion of the C/Cl-containing species due to thermal diffusion.

IV. RESULTS

Electron micrographs of diamond films grown on silicon (100) using 1% CH_2Cl_2 in H_2 and $CH_4/Cl_2/H_2$ in the ratio 1:1:98 as the input gases are shown in Fig. 5. Auger electron spectroscopy (AES) analysis of the as-grown diamond films indicated that high quality diamond was deposited using both the chlorocarbon precursors and $CH_4/Cl_2/H_2$ mixtures subject to the Cl atom input fraction being less than ~0.06. Small amounts of chlorine were detected on the surface of the diamond films, though no chlorine was detected in the bulk of the films. Higher concentrations of chlorine resulted in degradation of the diamond quality accompanied by significant

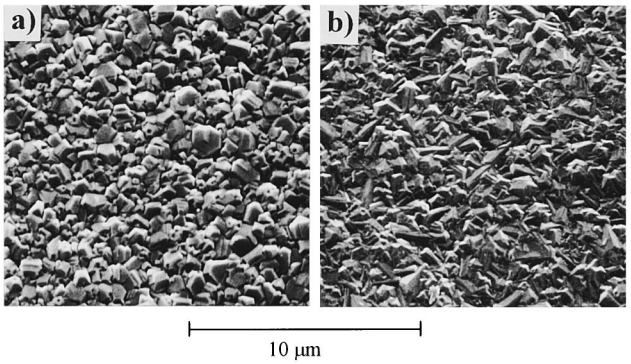

FIG. 5. Electron micrographs of diamond films grown on silicon using input gas mixtures of: a) 1% CH_2Cl_2 in H_2 and b) $CH_4/Cl_2/H_2$ in the ratio 1:1:98. Note that the chlorine concentration is 2 atom % for both precursor mixtures.

amounts of tantalum and chlorine impurities incorporated into the film. More detailed results of the AES analysis are reported elsewhere.[34]

A. Gas composition versus filament temperature for a variety of chlorine containing precursor gases in H_2

A series of quantitative measurements of the stable gas-phase species and CH_3 radicals was made using, respectively, chloromethane (CH_3Cl), dichloromethane (CH_2Cl_2), trichloromethane ($CHCl_3$) or tetrachloromethane (CCl_4) in H_2. The general product distributions as a function of filament temperature for all precursors show remarkable similarities. Figure 6 shows how such a distribution of the major stable product gases [CH_4 ($m/e=16$), C_2H_2 ($m/e=26$), and HCl ($m/e=36$ for $H^{35}Cl$)] vary as a function of filament temperature for an initial CH_2Cl_2/H_2 feedstock ratio of 1% measured 4 mm from the filament. Qualitatively, the plot reveals that the $CH_4/C_2H_4/C_2H_2$ product distribution as a function of temperature strongly resembles that obtained when methane is used as the precursor.[4] When the filament temperature is ~2100°C, methane is the dominant carbon containing species in the sampled gas, while at higher temperatures acetylene production becomes increasingly important. Furthermore, the absolute concentrations of the carbon- or chlorine-containing species in the vicinity of the filament diminish at higher temperatures due to thermal diffusion effects.

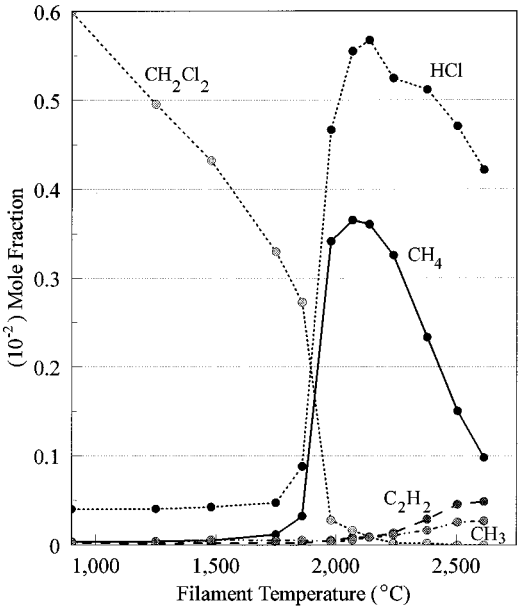

FIG. 6. Product distribution of major stable gas-phase species and methyl radicals as a function of filament temperature measured 4 mm from the filament using 1% CH_2Cl_2 in H_2 as input gas mixture. The species concentrations are presented with no correction being made as a result of thermal diffusion. The curve for C_2H_4 ($m/e = 28$) lies very close to that for CH_3, and so has been omitted for clarity.

Comparison of the observed trends in the relative gas concentrations of the hydrocarbon species using chlorine containing precursors with those found for CH_4/H_2 mixtures[4] suggest that a similar reaction mechanism is taking place, namely the chemical conversion of methane to acetylene as the filament temperature is increased, a reaction which is initiated by the dissociation of methane yielding methyl radicals:

$$CH_4 + H \rightarrow CH_3 + H_2. \tag{3}$$

Methyl recombination followed by successive H atom abstractions yields acetylene. As the filament temperature increases, the increasing H atom concentration drives the equilibrium from CH_4, through C_2H_6 and C_2H_4 to C_2H_2. No C_2H_6 was detected, because of its transient nature (and thus very low steady-state concentration) at high H atom concentrations, [H]. Quantitative measurements of the absolute concentrations of methyl radicals were made simultaneously and are displayed in Fig. 6. An increase in the filament temperature results in higher [CH_3] which is mirrored by increased [C_2H_2]. As with methane and other hydrocarbon precursor gases,[4] it is clear that the CH_3 radical is also an essential intermediate in the formation of acetylene when chlorine containing input precursors are used.

Inspection of Fig. 6 shows that the concentration of dichloromethane diminishes rapidly for filament temperatures above ~1700 °C as the relatively weak C-Cl bonds are broken in preference to C-H bonds by Cl abstraction with H atoms, e.g.,

$$\begin{aligned} &CH_2Cl_2 + H \rightleftharpoons CH_2Cl + HCl \\ &CH_2Cl + H \rightleftharpoons CH_2 + HCl, \quad \text{etc.} \end{aligned} \tag{4}$$

A corresponding rise in the HCl concentration is observed reaching a maximum value at the same temperature as methane (~2100°C). At this temperature almost all of the dichloromethane has been reduced. Similar trends were observed for all of the other $CH_{4-n}Cl_n$, ($n=1$–4) species, resulting in the reduction of the precursors to produce primarily methane and HCl, [see Figs. 7(a) and 7(b)]. Figure 7(c) shows how the acetylene concentrations vary as a function of filament temperature for input gas mixtures containing 1% $CH_{4-n}Cl_n$, ($n=0$–4) in H_2. For all the precursors, the C_2H_2 concentration rises sharply above ~2100°C as the H atom concentration increases. However, there is a significant increase in the C_2H_2 concentration for CCl_4 and, to a lesser extent, for $CHCl_3$ at lower temperatures (~1900–2100 °C).

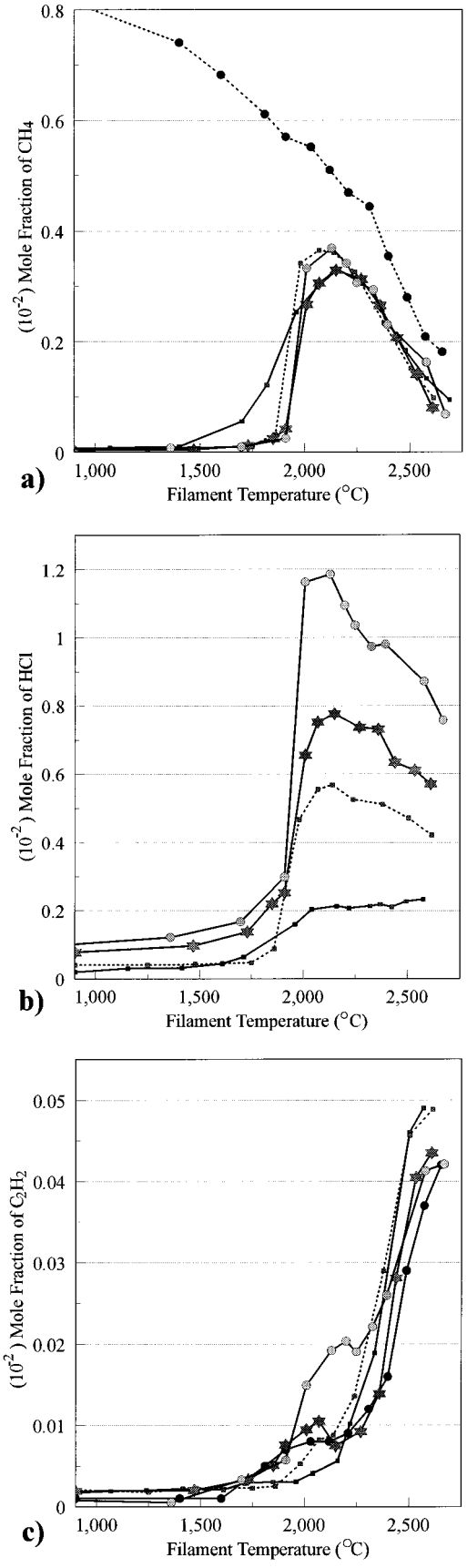

FIG. 7. Variation in concentration of the major stable species versus filament temperature: (a) methane, (b) HCl, and (c) acetylene, measured 4 mm from the filament starting with 1% each of CH_4 (---●---), CH_3Cl (—■—), CH_2Cl_2 (---■---), $CHCl_3$ (—✱—) or CCl_4(···※···) in H_2.

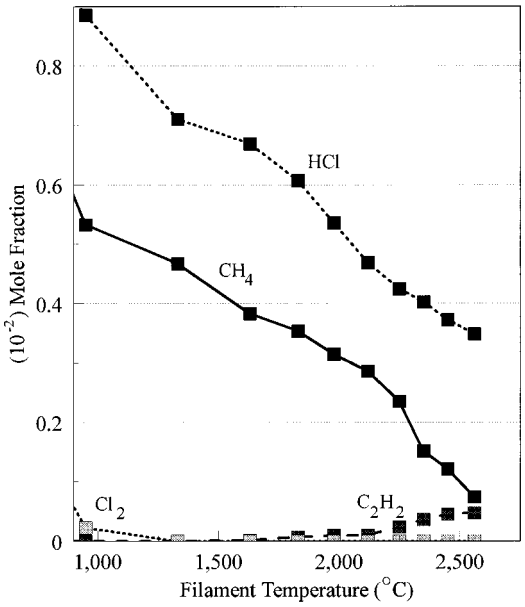

FIG. 8. Gas composition as a function of filament temperature measured 4 mm from the filament for a gas mixture of 1% CH_4 and 1% Cl_2 in H_2.

In the case of $CHCl_3$ for example, this might indicate the operation of a mechanism in which a single C-Cl bond is cleaved to form the $CHCl_2$ radical which could then combine with a CH_3 radical to produce $CHCl_2CH_3$. Subsequent elimination of two HCl molecules, reactions which are known to have reasonably low activation barriers,[35] would yield acetylene. We should point out, however, that we have not been able to detect this intermediate, possibly due to its instability in the presence of atomic hydrogen.

B. Gas composition versus filament temperature for various $CH_4/Cl_2/H_2$ gas mixtures

Similar measurements of the stable gas species were made using different $CH_4/Cl_2/H_2$ gas mixtures subject to the same process conditions as the chlorine containing hydrocarbon experiments. Figure 8 shows how the distribution of the major stable product gases [CH_4, C_2H_2, HCl and Cl_2 (m/e =70 for $^{35}Cl_2$)] change as a function of filament temperature for an initial $CH_4/Cl_2/H_2$ feedstock ratio of 1:1:98 measured 4 mm from the filament. Almost all the molecular chlorine is dissociated when the filament temperature is ~1000°C. The Cl atoms then undergo rapid reaction with hydrogen to form HCl,

$$Cl + H_2 \rightleftharpoons H + HCl. \tag{5}$$

The absolute measured concentrations of both HCl and methane decrease with temperature due to the thermal diffusion effects mentioned previously. At temperatures of ~2100°C and above there is a striking similarity in the measured C/Cl product distribution with that obtained with 1% CH_2Cl_2 in H_2 as the input gas mixture (cf. Fig. 6). In these two cases the relative C/Cl input mole fractions in H_2 are identical.

Figure 9 shows the temperature variation of: (a) [CH_4], (b) [C_2H_2] and (c) [HCl], for different input concentrations of Cl_2 (0%, 1%, 2%, 4%) in the CH_4/Cl_2 gas mixtures in

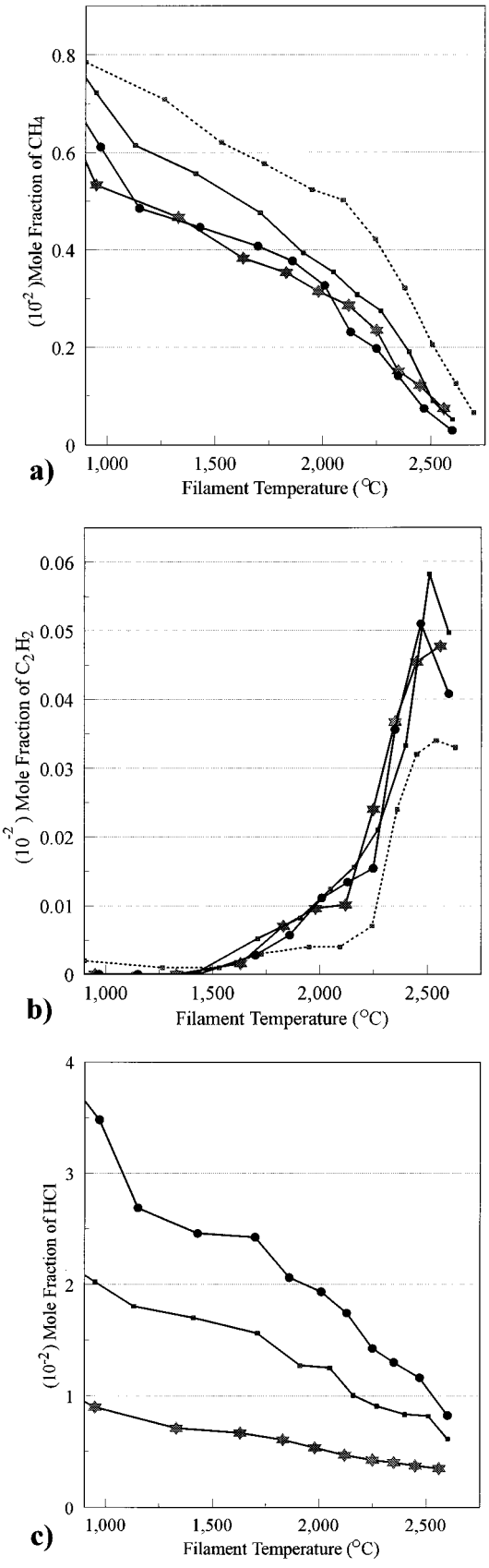

FIG. 9. Variation in concentration of the major stable species versus filament temperature: (a) methane, (b) acetylene and (c) HCl, measured 4 mm from the filament starting with 1% CH_4 in H_2 (----■----), then introducing 1% (—✱—), 2% (—■—) and 4% (—●—) Cl_2 respectively into the gas mixture.

H_2. As with the chlorine containing hydrocarbons the observed trends for the hydrocarbon species at and above filament temperatures $\sim$2100°C indicate that the reaction mechanism is congruent with that found for methane as the precursor, namely the chemical conversion of methane to acetylene via methyl recombination followed by successive H abstractions.

C. Gas composition versus filament temperature using 1% CF_4 in H_2

No significant concentrations of CH_4, C_2H_4, C_2H_2 or HF were detected at any filament temperature when using a 1:100 CF_4/H_2 mixture as the precursor. The difficulty in producing atomic fluorine or methyl radicals suggests that CF_4 is not a suitable precursor for diamond growth by HFCVD and, indeed, growth studies using CH_3F[14] in a hot filament reactor show much reduced growth rates. Further evidence that conditions are not suitable for diamond growth comes from the analysis of the tantalum filament after deposition. For all hydrocarbon precursors investigated thus far[3] and for the $CH_{4-n}Cl_n$ (n=1–4) species studied here, the filament carburizes and forms a stable gold colored tantalum carbide coating after a few minutes of deposition, indicating the presence of carbon radical species. In the case of CF_4 a grey film (presumably tantalum fluoride) forms on the filament and the filament temperature tends to be rather unstable. We note, however, that C/H/F gas mixtures have been used to grow diamond successfully by microwave plasma CVD, and MBMS studies[36] of such systems indicate that HF is the major sink for fluorine.

V. DISCUSSION

We have demonstrated that the technique of molecular beam mass spectrometry is able to provide quantitative measurements of both stable and free radical gas-phase species under conditions typical in the diamond CVD process. Due care has to be taken, however, in the data reduction procedures because the overall system sensitivity is critically dependent on the local temperature, pressure and composition of the gas being sampled. We have demonstrated that simple empirically based correction procedures can offset such variations in the sampling efficiency. Armed with a sensitive gas-phase analysis technique and the necessary data reduction procedures for the characterization of a CVD environment we turned our attention to the study of chlorine-assisted CVD of diamond.

As with the hydrocarbon precursor gases[5] chlorine containing hydrocarbons are reduced to methane at very similar temperatures, the other major product being hydrogen chloride which is formed in near stoichiometric amounts. At higher filament temperatures the temperature variation of the relative $CH_4/C_2H_4/C_2H_2$ product distribution generally mirrors that found for the hydrocarbon precursors at similar C/H_2 input ratios. Only with $CHCl_3$ or CCl_4 do we observe significant acetylene formation at considerably lower filament temperatures which may indicate the presence of transient chlorine-containing radical species supplementing the CH_3 radicals as precursors to acetylene formation.

TABLE II. Equilibrium and forward rate constants vs temperature.[a]

Reaction	log k_f T=500 K	800 K	1200 K	log K_{eq} T=500 K	800 K	1200 K
$H+HF\rightarrow H_2+F$	−0.7	5.2	8.4	−13.9	−8.6	−5.7
$H+HCl\rightarrow H_2+Cl$	11.7	12.2	12.5	0.2	0.03	−0.1
$H+CH_4\rightarrow CH_3+H_2$	8.9	11.0	12.1	1.0	1.2	1.4
$H+CH_3Cl\rightarrow CH_3+HCl$	9.6	11.0	12.2	9.9	6.8	5.0
$H+CH_3Cl\rightarrow CH_2Cl+HCl$				3.2	2.6	2.2
$Cl+CH_4\rightarrow CH_3+HCl$	11.7	12.1	12.8	0.8	1.2	1.4
$Cl+CH_3Cl\rightarrow CH_2Cl+HCl$	12.2	12.6	12.8	3.0	2.6	0.0

[a]See Reference 14.

Previous reports[14,15,20] have speculated upon the relative importance of (a) modification of the gas-phase chemistry enhancing the production of diamond precursor species, or (b) fast reaction of atomic hydrogen with surface bonded C-Cl and atomic Cl with surface bonded C-H which open up active surface growth sites at reduced substrate temperatures, as possible explanations for the observations that addition of small amounts of chlorine in the CVD process encourages diamond growth at lower substrate temperatures.

Our inability to detect the CH_2Cl radical in the present MBMS study suggests that its concentration must be at least an order of magnitude smaller than that of CH_3 at filament temperatures which produce optimum diamond growth ($\sim$2200–2400°C). This is presumably because the residual CH_4 concentration at these elevated temperatures is several times higher than that of CH_3Cl even when CH_3Cl is the input precursor; for dichloromethane and trichloromethane no significant concentration of CH_3Cl is measurable. This is to be expected since thermodynamic and kinetic arguments suggest that the C-Cl bond is likely to be broken in preference to the C-H bond. Therefore, we do not believe that gas-phase chemistry involving chlorohydrocarbon radicals can be primarily responsible for enhanced growth rates at lower substrate temperatures. However, it is possible that the addition of the CH_2Cl radical to the diamond surface and the subsequent elimination of HCl may occur more readily than addition of the CH_3 radical followed by elimination or successive abstraction of hydrogen at lower substrate temperatures.

At filament temperatures above $\sim$2000°C most of the chlorine is rapidly abstracted by H atoms from the parent chlorohydrocarbon to produce HCl in amounts proportional to the Cl mole fraction in the source gas. Similarly Cl_2 is almost entirely reduced to HCl at filament temperatures above 1000°C. However, in this case it is atomic chlorine produced by the thermal dissociation of Cl_2 which reacts rapidly with molecular hydrogen to form HCl. It has been proposed that the ability of chlorine to play a part in CVD diamond deposition stems from the interchangeability of atomic Cl with atomic H in an HCl/H_2 atmosphere. Calculations of Bai *et al.*[14] indicate that for the reaction,

$$H+HCl\underset{k_b}{\overset{k_f}{\rightleftharpoons}}Cl+H_2 \tag{6}$$

the equilibrium constant (K_{eq}) is close to unity over a large temperature range and the forward and backward rate constants (k_f and k_b) are large (see Table II), thereby allowing rapid equilibration at typical substrate temperatures. Therefore, the relative concentration ratio of Cl/H atoms is proportional to the Cl fraction in the source gas mixture regardless of the form of chlorine in the input mixture.

The MBMS results combined with the AES analysis[34] of the as-grown diamond films are consistent with the premise that Cl atoms play some part in gas surface reactions involved in the production of active surface growth sites at reduced substrate temperatures. Chemical kinetics calculations[20] have shown that the rate of H abstraction by Cl atoms from a (110) diamond surface at 670°C is some 60 times faster than abstraction by gas-phase H atoms. As indicated above, the Cl atom concentration at standard filament temperatures is directly related to the Cl fraction in the input gas, regardless of the form of the chlorine precursor. Our chlorine assisted diamond growth studies shows that if the Cl input fraction is too high (>0.06) the quality of the diamond grown at normal substrate temperatures ($\sim$900°C) is reduced, probably because a large fraction of surface sites are activated, leading to the graphitization of the diamond surface. These findings broadly agree with the diamond growth domain indicated in the C/H/Cl ternary gas-phase composition diagram of Bachmann *et al.*[37] However, at lower substrate temperatures the presence of such chlorine concentrations in the process gas mixture would result in an increased deposition rate due to the greater efficiency of surface hydrogen abstraction by Cl atoms.

The inability of fluorine containing precursors to participate in the hot filament CVD of diamond results from the strength of the C-F bond. Our gas-phase composition findings when using 1% CF_4 in H_2 indicate that very little CH_4 or HF are produced; further, even if we could produce atomic fluorine, the equilibrium

$$H + HF\rightleftharpoons H_2 + F \tag{7}$$

lies far to the left in a hydrogen atmosphere (see Table II).

ACKNOWLEDGMENTS

C.A.R., P.W.M. and M.N.R.A. thank the Royal Society for financial support. We also thank Dr. N. M. Everitt of the Department of Aerospace Engineering, University of Bristol for helpful discussions and Dr. C. M. Younes of the Interface Analysis Centre, University of Bristol for the Auger analysis.

[1] F. G. Celii and J. E. Butler, Annu. Rev. Phys. Chem. **42**, 643 (1991), and references therein.
[2] M. N. R. Ashfold, P. W. May, C. A. Rego, and N. M. Everitt, Chem. Soc. Rev. **23**, 21 (1994).
[3] C-H. Wu, M. A. Tamor, T. J. Potter, and E. W. Kaiser, J. Appl. Phys. **68**, 4825 (1990).
[4] C. A. Rego, P. W. May, C. R. Henderson, M. N. R. Ashfold, K. N. Rosser, and N. M. Everitt, Diamond Relat. Mater. **4**, 770 (1995).
[5] M. C. McMaster, W. L. Hsu, M. E. Coltrin, D. S. Dandy, and C. Fox, Diamond Relat. Mater. **4**, 1000 (1995).
[6] M. Tsuda, M. Nakajima, and S. Okinawa, J. Am. Chem. Soc. **108**, 5780 (1986).
[7] S. J. Harris, Appl. Phys. Lett. **56**, 2298 (1990).
[8] M. Frenklach and K. E. Spear, J. Mater. Res. **3**, 133 (1988).
[9] S. Skokov, B. Weiner, and M. Frenklach, J. Phys. Chem. **98**, 8 (1994).
[10] Y. Hirose and Y. Terasawa, Jpn. J. Appl. Phys. **25**, L519 (1986).
[11] Y. Saito, K. Sato, K. Gomi, and H. Miyadera, J. Mater. Sci. **25**, 1246 (1990).
[12] T. Kawato and K. Kondo, Jpn. J. Appl. Phys. **26**, 1429 (1986).
[13] P. K. Bachmann, D. Leers, and H. Lydtin, Diamond Relat. Mater. **1**, 12 (1991).
[14] B. J. Bai, C. J. Chu, D. E. Patterson, R. H. Hague, and J. L. Margrave, J. Mater. Res. **8**, 233 (1993).
[15] F. C.-N. Hong, G.-T. Liang, J.-J. Wu, D. Chang, and J.-C. Hsieh, Appl. Phys. Lett. **63**, 3149 (1993).
[16] F. C.-N. Hong, J.-J. Wu, C.-T. Su, and S.-H. Yeh, in *Advances in New Diamond Science and Technology* (MYU, Tokyo, 1994), p. 85.
[17] C. H. Chu and M. H. Hon, Diamond Relat. Mater. **2**, 311 (1993).
[18] T. Nagano and N. Shibata, Jpn. J. Appl. Phys. **32**, 5067 (1993).
[19] C. Pan, C. J. Chu, J. L. Margrave, and R. H. Hague, J. Electrochem. Soc. **141**, 3246 (1994).
[20] N. J. Komplin, B. J. Bai, C. J. Chu, J. L. Margrave, and R. H. Hague, in *Diamond Materials* (The Electrochemical Society, Pennington, NJ, 1993), Vol. 93-17, p. 385.
[21] *Tables of Physical and Chemical Constants*, edited by G. W. C. Kaye and T. H. Laby (Wiley, New York, 1989).
[22] S. J. Harris and A. M. Weiner, J. Appl. Phys. **67**, 6520 (1990).
[23] S. J. Harris, A. M. Weiner, and T. A. Perry, Appl. Phys. Lett. **53**, 1605 (1989).
[24] S. J. Harris, D. N. Belton, A. M. Weiner, and S. J. Schmieg, J. Appl. Phys. **66**, 5353 (1989).
[25] R. Beckmann, B. Sobisch, and W. Kulisch, Ref. 20, p. 1026.
[26] I. Schmidt, C. Benndorf, and P. Joeris, Diamond Relat. Mater. **4**, 725 (1995).
[27] W. L. Hsu and D. M. Tung, Rev. Sci. Instrum. **63**, 4138 (1992).
[28] W. L. Hsu, J. Appl. Phys. **72**, 3102 (1992).
[29] W. L. Hsu, M. C. McMaster, M. E. Coltrin, and D. S. Dandy, Jpn. J. Appl. Phys. **33**, 2231 (1994).
[30] C. A. Rego, P. W. May, C. R. Henderson, M. N. R. Ashfold, K. N. Rosser, and N. M. Everitt, *New Diamond Science and Technology* (MYU, Tokyo, 1994), p. 485.
[31] H. Chatham, D. Hils, R. Robertson, and A. Gallagher, J. Chem. Phys. **81**, 1770 (1984).
[32] D. P. Wang, L. C. Lee, and S. K. Srivastava, J. Chem. Phys. **152**, 513 (1988).
[33] R. B. Bird, W. E. Stewart, and E. N. Lightfoot, *Transport Phenomena* (Wiley, New York, 1960), p. 567.
[34] R. S. Tsang, C. A. Rego, P. W. May, J. Thumim, M. N. R. Ashfold, K. N. Rosser, C. M. Younes, and M. J. Holt, Diamond Relat. Mater. (in press).
[35] W. Ho, R. B. Barat, and J. W. Bozzelli, Combust. Flame **88**, 265 (1992).
[36] C. Fox and W. L. Hsu (private communication).
[37] P. K. Bachmann, H. J. Hagemann, H. Lade, D. Leers, F. Picht, D. U. Wiechert, and H. Wilson, Mater. Res. Soc. Symp. Proc. **339**, 267 (1994).